Membrane Protein Frustration: Protein Incorporation into Hydrophobic Mismatched Binary Lipid Mixtures

David Stopar,[†] Ruud B. Spruijt,[‡] and Marcus A. Hemminga[‡*]

[†]University of Ljubljana, Biotechnical Faculty, Ljubljana, Slovenia; and [‡]Laboratory of Biophysics, Wageningen University, Wageningen, The Netherlands

ABSTRACT   Bacteriophage M13 major coat protein was reconstituted in different nonmatching binary lipid mixtures composed of 14:1PC and 22:1PC lipid bilayers. Challenged by this lose-lose situation of hydrophobic mismatch, the protein-lipid interactions are monitored by CD and site-directed spin-label electron spin resonance spectroscopy of spin-labeled site-specific single cysteine mutants located in the C-terminal protein domain embedded in the hydrophobic core of the membrane (I39C) and at the lipid-water interface (T46C). The CD spectra indicate an overall α-helical conformation irrespective of the composition of the binary lipid mixture. Spin-labeled protein mutant I39C senses the phase transition in 22:1PC, in contrast to spin-labeled protein mutant T46C, which is not affected by the transition. The results of both CD and electron spin resonance spectroscopy clearly indicate that the protein preferentially partitions into the shorter 14:1PC both above and below the gel-to-liquid crystalline phase transition temperature of 22:1PC. This preference is related to the protein tilt angle and energy penalty the protein has to pay in the thicker 22:1PC. Given the fact that in *Escherichia coli*, which is the host for M13 bacteriophage, it is easier to find shorter 14 carbon acyl chains than longer 22 carbon acyl chains, the choice the M13 coat protein makes seems to be evolutionary justified.

INTRODUCTION

Phospholipids are the main constituents of biological membranes. Apart from differences in the polar headgroup, membrane phospholipids display a very large range of different hydrophobic acyl chains with respect to length and degree of saturation (1). The hydrophobic chain length of phospholipids controls the thickness of the bilayers and thereby may control the activity of embedded membrane proteins. For example, the hydrophobic thickness of the bilayer regulates the activity of the ion channel gramicidin A (2) and the activity of the Ca^{2+}-ATPase and other membrane transporters (3,4). For phospholipids with the same headgroup, a next level of complexity arises by considering the gel-to-liquid crystalline phase transition from a two-dimensional crystalline solid with lipid acyl chains of high conformational order to a two-dimensional fluid (liquid) in which the acyl chains of the lipid molecules have a high degree of conformational disorder (5). In the case of binary mixtures of phospholipids with the same headgroup, the two-dimensional structure can be further modified by introducing small amounts of a third amphiphilic component, which can mediate the boundaries between phase-separated regions. This third component can conveniently be selected as a phospholipid molecule with an acyl chain

length in between the ones of the majority species and can act as a surfactant (6). Instead, a membrane protein with a hydrophobic length in between the ones of the lipid species could relieve the frustration arising from mismatch of the chain lengths of the phospholipids. For example, in a mixture of 14:1PC and 24:1PC, Ca^{2+}-ATPase binds two Ca^{2+} ions, compared with one in either 14:1PC or 24:1PC alone, and the ATPase activity is also higher, showing that a suitable combination of short and long phospholipids can produce a membrane equivalent to that produced by 18:1PC, the phospholipid of optimal structure (7).

In this work, the major coat protein of bacteriophage M13 was reconstituted into different nonmatching binary lipid mixtures composed of 14:1PC and 22:1PC lipid bilayers. This transmembrane protein was selected as a model protein, because it has been the subject of numerous biophysical studies in bilayers of different polar headgroups and chain lengths and its structure and topology in the mono- and binary lipid bilayer mixtures is well documented (for a review, see Stopar and colleagues (8,9)). It has also been shown that in binary lipid mixtures of different chain lengths, where one of the lipids selected was a matching lipid, the coat protein is preferentially surrounded by the matching 18:1PC (10). This finding is not unexpected because the protein avoids the hydrophobic penalty imposed on it by a hydrophobic mismatch (for a review, see Marsh (11)). In a real host membrane, however, the coat protein is likely to encounter nonmatching lipids both longer and shorter than the hydrophobic thickness of the embedded transmembrane protein (12). If the protein is challenged by a lose-lose situation, as in binary mixtures composed of 14:1PC and 22:1PC, the physicochemical behavior of the protein is

---

Abbreviations used: 14:1PC, 1,2-dimyristoleoyl-*sn*-glycero-3-phosphocholine; 18:1PC, 1,2-dioleoyl-*sn*-glycero-3-phosphocholine; 20:1PC, 1,2-dieicosenoyl-*sn*-glycero-3-phosphocholine; 22:1PC, 1,2-dierucoyl-*sn*-glycero-3-phosphocholine; 24:1PC, 1,2-dinervonoyl-*sn*-glycero-3-phosphocholine; CD, circular dichroism; ESR, electron spin resonance; L/P, lipid/protein molar ratio.

difficult to predict. It may partition into one or the other lipid domain, or it may act as a ''mediator'', positioning itself at the lateral borders of the lipid domains to relieve the tension at the interface and thereby acting as a surfactant. Provoked by this problem, we used CD spectroscopy and selected two coat protein mutants for site-directed spin-label ESR spectroscopy, with one mutant having the spin-labeled site embedded within the hydrophobic core of the membrane (I39C), and one positioned at the C-terminal protein domain in the lipid-water interface (T46C). In our experiments, we challenged the protein with a ''molecular frustration'' (13) arising from its opposing preferences for two unfavorable hydrophobic mismatched situations.

MATERIAL AND METHODS

Sample preparation

Site-specific single cysteine mutants I39C and T46C of bacteriophage M13 major coat protein were prepared, purified, and labeled with 3-maleimidoproxyl spin label (Aldrich, St. Louis, MO), as described previously (14,15). Labeled mutants were reconstituted into 14:1PC and 22:1PC bilayers (all lipids purchased from Avanti Polar Lipids, Alabaster, AL) at L/P 100, as reported earlier (14,16,17). Lipid bilayers were prepared with the following mol/mol ratios of 14:1PC to 22:1PC: 0/100, 20/80, 40/60, 60/40, 80/20, and 100/0. All lipid mixtures were prepared at room temperature, which is well above the phase transition of the lipids (i.e., $-4°C$ for 14:1PC (18) and $12°C$ for 22:1PC (19)). For the purpose of ESR measurements, the proteoliposomes were then concentrated using lyophilization and subsequent rehydration, and finally, the multilamellar protein-containing vesicles were collected by high-speed centrifugation (20).

CD measurements

CD measurements were performed at room temperature on a Jasco J-715 spectropolarimeter (Jasco, Easton, MD) in the wavelength range of 190–250 nm using a 1 mm path length. The CD settings were 100 s scan time, 1 nm bandwidth, 0.1 nm resolution, and 125 ms response time. Up to 50 spectra were accumulated to improve the signal/noise ratio. CD spectra of 3-maleimidoproxyl spin-labeled M13 coat protein mutant I39C reconstituted using the cholate dialysis reconstitution procedure (16) in each binary 14:1PC and 22:1PC lipid mixture, and their respective background spectra, were recorded in 100 mM sodium phosphate buffer (pH 8.0) under the same experimental conditions. Difference spectra were obtained by subtracting the background spectra from the corresponding spectra. For the purpose of comparison, the different CD spectra were normalized to the same intensity at 222 nm.

ESR spectroscopy

Samples of reconstituted spin-labeled 3-maleimidoproxyl spin-labeled M13 coat protein mutants I39C and T46C in different binary 14:1PC and 22:1PC lipid mixtures were filled up to 5 mm in 50 μL glass capillaries that were accommodated within standard 4 mm diameter quartz tubes. ESR spectra were recorded at room temperature on a Bruker ESP 300E ESR spectrometer (Bruker, Rheinstetten, Germany) equipped with a 108TMH/9103 microwave cavity. The ESR settings were 6.38 mW microwave power, 0.1 mT modulation amplitude, 40 ms time constant, 80 s scan time, 10 mT scan range, and 338.9 mT center field (21–24). Up to 20 spectra were collected to improve the signal/noise ratio. The temperature was controlled with a temperature control unit (Eurotherm temperature control, Eurotherm, Leesburg,VA). Each sample was equilibrated at a given temperature for 5 min before the ESR spectra were recorded.

RESULTS

CD spectroscopy

Fig. 1 shows the CD spectra of the protein mutant I39C labeled with the 3-maleimidoproxyl spin label and reconstituted in different binary 14:1PC and 22:1PC lipid mixtures at room temperature, well above the temperature of the main phase transition for both lipids (18,19). The CD spectra suggest an overall α-helical conformation irrespective of the composition of the binary lipid mixture. Nevertheless, small differences in the CD spectra can be observed. The negative ellipticity at 210 nm increases from 22:1PC to 14:1PC, with increasing molar fraction of 14:1PC in the binary mixture. For the protein reconstituted in 22:1PC, the zero crossing of the ellipticity is shifted to a slightly higher wavelength. However, in CD spectra there is no indication of an irreversible β-sheet aggregation for the protein (23). The ratio R of the ellipticity at 210 and 222 nm is
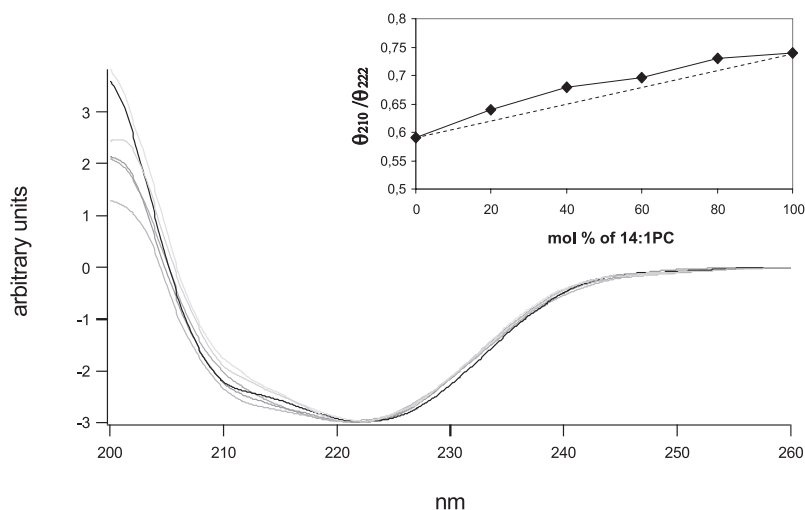

FIGURE 1 CD spectra of 3-maleimidoproxyl spin-labeled M13 coat protein mutant I39C reconstituted in multilamellar vesicles composed of binary 14:1PC and 22:1PC lipid mixtures at different molar ratios, at L/P 100 in 100 mM sodium phosphate buffer (pH 8.0) and at room temperature. The CD spectra were normalized to the same intensity at 222 nm. An increasing fraction of 14:1PC is indicated with an increasing shade of gray. The inset shows the ratio of the ellipticity at 210 and 220 nm as a function of lipid composition.

plotted in the inset of Fig. 1. The ratio of the ellipticities increases nonlinearly, with increasing molar fraction of 14:1PC in the lipid binary mixtures.

ESR experiments

Typical ESR spectra of the spin-labeled protein mutant I39C reconstituted in different binary 14:1PC and 22:1PC lipid mixtures are presented in Fig. 2. The spectra were recorded at a temperature of 275 K, which is above the main gel-to-liquid crystalline phase transition of 14:1PC (269 K), but below the main phase transition of 22:1PC (285 K). All ESR spectra have a composite appearance, showing a broad immobile spectrum and a relatively sharp mobile component. The immobile spectrum can be characterized by the outer hyperfine splitting A_{out}, which decreases from 6.62 to 6.18 mT upon increasing amounts of 14:1PC in the binary lipid mixtures. The outer hyperfine splitting is an indication of the local order of the spin label (25,26). The small mobile spectral component with a hyperfine splitting of 1.6 mT is attributed to nonspecific spin labeling (21).

For the spin-labeled protein mutants I39C and T46C, the dependence of the outer hyperfine splitting on the temperature in the different binary lipid mixtures is shown in Fig. 3. Clearly, the spin-labeled moieties of the protein mutants feel the changes in the protein-lipid environment, which is reflected by a decrease of the outer hyperfine splitting on increasing temperature. When the spin-labeled protein mutant I39C is reconstituted in pure 22:1PC (Fig. 3 A), the outer hyperfine splitting A_{out} shows a small drop at the main lipid phase transition temperature around 285 K. With the addition of 20 mol % of 14:1PC, this effect is gone. For higher amounts of 14:1PC, the temperature dependence of the outer hyperfine splitting becomes similar to that of pure 14:1PC and decreases linearly with increasing temperature. Clearly, there is no phase transition observed for the spin-labeled protein mutant I39C in pure 14:1PC in the temperature range studied, in agreement with a main phase transition temperature of 14:1PC of 269 K. The decrease of the outer hyperfine splitting

with increasing temperature is 35 μT/K for pure 14:1PC. In 22:1PC, the gradient is ~17 μT/K, below and above the lipid phase transition temperature (Table 1).

In contrast, no phase transition can be observed for the spin-labeled protein mutant T46C in all binary lipid mixtures studied (Fig. 3 B). As in the case of mutant I39C, the addition of 14:1PC reduces the outer splitting. The decrease of the outer hyperfine splitting with increasing temperature in pure 22:1PC and 14:1PC is 36 and 32 μT/K, respectively (Table 1).

DISCUSSION

The physicochemical properties of the bacteriophage M13 major coat protein reconstituted in binary lipid mixtures composed of nonmatching 14:1PC and 22:1PC lipid bilayers have been investigated by CD and site-directed spin-label ESR spectroscopy of protein mutants at different temperatures. For our study, we selected two typical mutants located in the C-terminal domain of the transmembrane α-helix of the protein (9,26–29). When embedded in the lipid bilayer, the spin label of mutant I39C is located at the proximal end of the hydrophobic lipid acyl chains, whereas the spin label of mutant T46C is located in the phospholipid head-group region at the lipid-water interface. In general, lipid bilayer membranes composed of two types of phospholipids with different chain lengths have a common binary phase diagram. The phase diagram displays a uniform liquid crystalline phase at high temperature and coexisting solid and liquid crystalline phases between the chain-melting temperatures of the two components (30). In our ESR work, we equilibrated the samples for 5 min at each temperature, thereby avoiding nonequilibrium effects on our protein-lipid systems as much as possible. Therefore, we assume that below the first main phase transition of 22:1PC, relatively small domains of lipids are present, consisting of fluid and gel-like lipids (<600 lipid molecules per domain) (31).

As shown by the CD spectra in Fig. 1, the overall secondary structure of the protein in both pure 14:1PC and
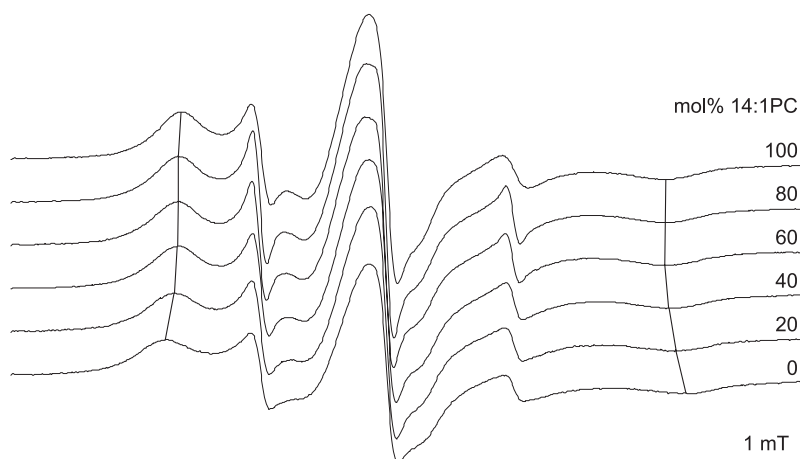

mol% 14:1PC

100

80

60

40

20

0

1 mT

FIGURE 2 ESR spectra of 3-maleimidoproxyl spin-labeled M13 coat protein mutant I39C reconstituted in multilamellar vesicles composed of binary 14:1PC and 22:1PC lipid mixtures at different molar ratios, at L/P 100 in 100 mM sodium phosphate buffer (pH 8.0) and at 275 K. Spectral line heights are normalized to the same integral intensity. The total horizontal scan range is 10 mT. The vertical solid lines indicate the outer hyperfine splitting A_{out}.
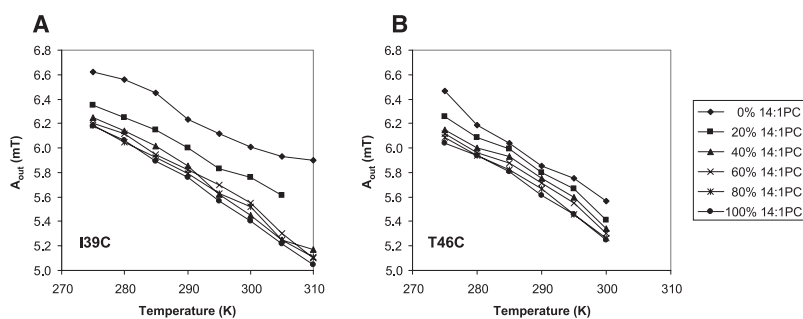
FIGURE 3 Temperature dependence of the outer hyperfine splitting (A_{out}) of 3-maleimidoproxyl spin-labeled M13 coat protein mutants I39C (*A*) and T46C (*B*) reconstituted in multilamellar vesicles composed of 14:1PC and 22:1PC binary lipid mixtures at different molar ratios at L/P 100.

22:1PC lipid bilayers is mainly α-helical. We analyzed the CD data using the ratio $R = \theta_{210}/\theta_{222}$, where θ_{210} and θ_{222} are the ellipticities at 210 and 222 nm, respectively. For a random structure, R is close to zero, and in a highly helical state, R will approach 1 (32). It can be seen in the inset of Fig. 1 that R increases upon an increasing fraction of 14:1PC in the lipid binary mixtures. As indicated by the ratios of 0.60 and 0.75 in the inset of Fig. 1, the overall secondary structure of the protein in both pure 14:1PC and 22:1PC lipid bilayers is mainly α-helical. However, the difference shows that the protein as a whole adopts two slightly different secondary structures in 14:1PC and 22:1PC. Based on this analysis of the CD spectra, it is not possible to assign the locations of the structure changes. However, as demonstrated earlier, secondary structure changes in pure mismatched lipid bilayers are confined mostly to the N-terminal amphipathic helix (26,29). If the protein did not show any preference for either short or long lipids, one would expect that in binary mixtures, ratio R would be a linear function of the amount of 14:1PC, as indicated by the dotted line in the inset. Because this ratio is independent of inaccuracies in the determined protein concentration, as well as those caused by small shifts in wavelength (32), we can conclude that the experimental values are significantly above this equipartition line. This finding is a strong indication that in lipid binary mixtures, the protein as a whole does not equipartition into the two lipids but adopts a secondary structure that resembles the secondary structure of the protein in the shorter 14:1PC.

As can be seen in Fig. 3 *A*, a major change in the outer hyperfine splitting of the spin-labeled protein mutant I39C at any given temperature occurs upon introduction of 20 mol % of 14:1PC into 22:1PC (i.e., from 6.62 to 6.35 mT at 275 K). Upon a further increase of the fraction of 14:1PC in the binary mixture, the outer hyperfine splitting

of the spin-labeled protein mutant I39C side chain steadily decreases, but the relative effect is much smaller. From the ESR data it therefore follows that the protein prefers 14:1PC to 22:1PC. In the case of spin-labeled protein mutant T46C (Fig. 3 *B*), the reduction of the outer hyperfine splitting is strongest with the addition of 20 mol % of 14:1PC into 22:1PC, but this effect is much smaller than in the case of mutant I39C.

It is remarkable that the outer hyperfine splitting is so strongly temperature dependent (Table 1). This arises from the fact that the spin label side chain at the protein mutants is not only sensitive to the local environment, as provided by the neighboring amino acid residues and secondary structure of the protein, but also affected by the local lipid environments, which are for position 39 the CH_2 groups of the acyl chains, and the phospholipid headgroup atoms for position 46. The relatively high values for the outer hyperfine splitting for mutant I39C, as compared with the values found for mutant T46C, indicate that the local packing in the hydrophobic core of the lipid bilayer, as sensed by the spin label, is higher than at the lipid-water interface. This effect of a higher packing in the hydrophobic core of the membrane is supported by the reduced value of the gradient found for spin-labeled protein mutant I39C in pure 22:1PC (17 μT/K, as compared with 36 μT/K for mutant T46C). This finding indicates stronger intermolecular interactions in the proximal end of the hydrophobic lipid acyl chains as compared with the polar headgroup region. In the more fluid environment of 14:1PC, the corresponding gradients are 35 and 32 μT/K for spin-labeled protein mutants I39C and T46C, respectively. This analysis also explains the fact that spin-labeled protein mutant I39C senses the phase transition in 22:1PC, whereas spin-labeled protein mutant T46C is not affected by this. This finding is in agreement with those from the literature that in the gel state, the headgroups maintain a high degree of mobility (33). Consequently, we see a gradual decrease in the outer hyperfine splitting of spin-labeled protein mutant T46C with increasing temperature, and not an abrupt change (i.e., phase transition) as found for spin-labeled protein mutant I39C. At the same absolute temperature, the area per lipid decreases with increasing acyl chain length. In other words, on average, longer acyl chains keep the headgroups closer together (34), leading to a higher local

TABLE 1 Temperature gradient of the outer hyperfine splitting A_{out} (in μT/K) for 3-maleimidoproxyl spin-labeled M13 coat protein mutants I39C and T46C in 14:1PC and 22:1PC

	Mutant I39C	Mutant T46C
14:1PC	35	32
22:1PC	17	36

packing, which explains why in the presence of the same phospholipid headgroup, spin-labeled protein mutant T46C has a larger outer hyperfine splitting in 22:1PC than in 14:1PC. As can be seen from Table 1, the temperature gradient of the outer hyperfine splitting is most affected by the acyl chain length of the phospholipid for spin-labeled protein mutant I39C, which is in agreement with the observation that the main effect of increasing the number of acyl segments is on the hydrocarbon thickness rather than on the interfacial area (34).

From a topological point of view of the protein reconstituted in lipid bilayer, the major difference between 14:1PC and 22:1PC is the tilt angle of the protein (27). To accommodate in the short lipid bilayer, the protein has to tilt relative to the bilayer normal. In a thin lipid bilayer, the tilt angle is estimated to be around 33°, whereas in 20:1PC, it is around 19° (27), and it is expected to be even smaller in 22:1PC. A tilt of M13 coat protein in a lipid bilayer is only possible if it has anchoring points located at the lipid-water interface region. Such points are provided by a strong anchor in the C-terminus and a much weaker anchor in the N-terminal protein domain. The strong anchor is provided by the two phenylalanines (Phe-42 and Phe-45) and the three lysines (Lys-40, Lys-43, and Lys-44) at the C-terminal domain of the coat protein. A weak ''sliding'' anchor is provided by the hinge region of the protein and part of the N-terminal helix (9). The strong C-terminal anchor ensures that the position of the spin-labeled protein mutant T46C is not shifting more than 2 Å in 14:1PC as compared with 22:1PC (27). In conclusion, although the spin-labeled protein mutant molecules are almost identical (apart from their spin-labeled sites) and thus will have identical physical characteristics in their protein-lipid interactions, the spin label side chains at both labeling sites sense quite a different environment that is related to the physical state of the phospholipids.

There is no indication from the ESR spectra (Fig. 2) of the presence of two distinct slow-motional components in lipid binary mixtures that would arise from the protein residing in either 14:1PC or 22:1PC. This finding indicates that exchange of the protein between the two lipid environments is fast on the ESR timescale (~10^{-8} s). Fast exchange can be estimated in the following way. The lateral diffusion constant of the protein in 18:1PC has been reported previ-

ously to be 7.0×10^{-8} cm^2 s^{-1} (10), which gives a root mean-square displacement during the ESR lifetime of 53 nm. If we assume that the domain size in 14:1/22:1PC is similar to binary lipid mixtures composed of saturated phospholipids (dimyristoyl phosphatidylcholine and distearoyl phosphatidylcholine) (31), the average center-to-center distance for circular domains is ~20 nm, which, in principle, enables protein diffusion across the domain boundary and exchange between the two lipid environments. Furthermore, if the protein was then equally distributed over both lipids in the binary 14:1PC and 22:1PC lipid mixture, one would expect that the outer hyperfine splitting A_{out} should reflect the relative fraction of the two lipids in the mixture. However, the measured outer hyperfine splitting in the different binary lipid mixtures does not behave like this. A small increase in the fraction of 14:1PC reduces the outer hyperfine splitting the spin-labeled protein mutant I39C out of proportion (Fig. 3 A). In fact, at 14:1PC contents above 50 mol %, almost all contribution to the outer hyperfine splitting in Fig. 3 A can be explained by the protein partitioning into 14:1PC.

To describe this effect quantitatively and enable a comparison between spin-labeled protein mutants I39C and T46C, we define the normalized ratio f of the difference in the outer splittings as

$$f = \frac{A_{out}^{22:1PC} - A_{out}}{A_{out}^{22:1PC} - A_{out}^{14:1PC}}. \tag{1}$$

Here, $A_{out}^{14:1PC}$ and $A_{out}^{22:1PC}$ are the outer splittings in pure 14:1PC and 22:1PC, and A_{out} is the outer splitting in a given binary mixture. For both spin-labeled protein mutants at temperatures of 275, 290, and 310 K, ratio f is shown in Fig. 4 for each binary lipid mixture. For a random distribution of the protein over both lipids, a linear dependence would be expected, which is indicated by a dotted ''equipartitioning'' line in Fig. 4, similar to that shown in the inset of Fig. 1.

For the spin-labeled protein mutant I39C, all values for f are above this equipartitioning line, demonstrating that the protein preferentially partitions in 14:1PC (Fig. 4 A). This finding is consistent with the conclusions from the analysis of the CD data in Fig. 1. Furthermore, the preference for the protein to preferentially partition into 14:1PC over 22:1PC is in agreement with previous findings on the relative association
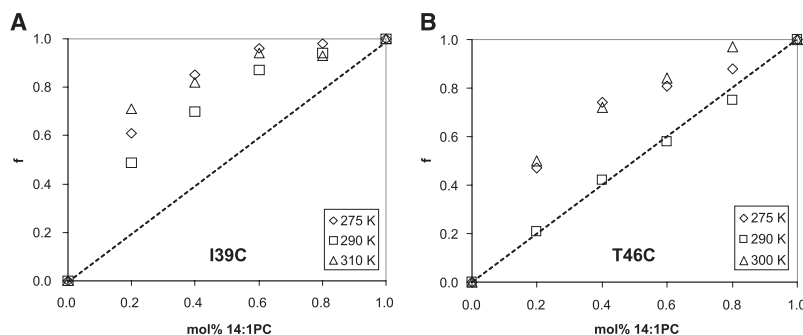

FIGURE 4   Plot of parameter f (see Eq. 1) of 3-maleimidoproxyl spin-labeled M13 coat protein mutants I39C (A) and T46C (B) as a function of 14:1PC content in binary 14:1PC and 22:1PC lipid mixtures at different temperatures. The dotted line represents the equipartitioning line (see text).

constants measured by fluorescence resonance energy transfer of the phospholipid fluorescent probe $(18:1)_2$-PE-NBD in unsaturated phosphatidylcholine bilayers of different acyl chain lengths (35). For spin-labeled protein mutant T46C (Fig. 4 B), however, the situation is different. The addition of 20 mol % of 14:1PC has a less pronounced effect on the partitioning than for mutant I39C. In addition, around the phase transition temperature of 22:1PC (285 K), the spin-labeled protein mutant T46C is equipartitioning in both lipids, which is not the case for the spin-labeled protein mutant I39C. The absence of equipartitioning of I39C mutant at the phase transition temperature of 22:1PC lipid and the larger partitioning in 14:1PC at smaller fractions of 14:1PC support the idea explained above that the spin label side chains in the two mutants experience a different physicochemical behavior in the binary lipid mixtures. Small differences between Fig. 4 A and B are attributed to the different location of the spin labels, with mutant I39C in the core of the membrane and mutant T46C in the headgroup region. Because the molecular packing in the headgroup region is different from that in the acyl chain region, the constraints of the local environment on the spin label are different. It is not surprising that because of the differences in these membrane domains, the spin labels will pick up different effects. The only exception is that around the phase transition temperature of 22:1PC, mutant T46C deviates in equipartitioning in the lipid mixtures. This effect may be related to anomalous effects of the protein at the phase transition of the phospholipids that have been found earlier in the literature and have been ascribed to an enhanced lateral compressibility of the lipid during phase transition (36).

It is not unusual that proteins show a clear preference for a particular lipid phase. For coexisting liquid and solid phases in model bilayers, a peptide or protein that is anchored to the membrane by an α-helix typically prefers the liquid phase (37,38). In this respect, the major coat protein is no exception. Below the phase transition of 22:1PC it is mostly found in 14:1PC. However, the protein is driven into 14:1PC even above the phase transition of 22:1PC, which suggests that there is another reason for partitioning. We believe that this is related to the protein tilt angle and energy penalty the snorkeling C-terminal lysines of the protein have to pay in the thicker 22:1PC phospholipid system (39). Given the fact that in *Escherichia coli*, which is the host for M13 bacteriophage, it is easier to find shorter 14 carbon acyl chain than longer 22 carbon acyl chain (12), the choice the M13 coat protein makes seems to be evolutionary justified.

REFERENCES

1. Kleinschmidt, J. H., and L. K. Tamm. 2002. Structural transitions in short-chain lipid assemblies studied by ^{31}P-NMR spectroscopy. *Biophys. J.* 83:994–1003.

2. Galbraith, T. P., and B. A. Wallace. 1999. Phospholipid chain length alters the equilibrium between pore and channel forms of gramicidin. *Faraday Discuss.* 111:159–164.

3. Cornea, R. L., and D. D. Thomas. 1994. Effects of membrane thickness on the molecular dynamics and enzymatic activity of reconstituted Ca-ATPase. *Biochemistry.* 33:2912–2920.

4. Dumas, F., J. F. Tocanne, G. Leblanc, and M. C. Lebrun. 2000. Consequences of hydrophobic mismatch between lipids and melibiose permease on melibiose transport. *Biochemistry.* 39:4846–4854.

5. Mouritsen, O. G. 1991. Theoretical models of phospholipid phase transitions. *Chem. Phys. Lipids.* 57:179–194.

6. Nielsen, L. K., A. Vishnyakov, K. Jørgensen, T. Bjørnholm, and O. G. Mouritsen. 2000. Nanometre-scale structure of fluid lipid membranes. *J. Phys. Condens. Matter.* 12:A309–A314.

7. Lee, A. G. 2003. Lipid-protein interactions in biological membranes: a structural perspective. *Biochim. Biophys. Acta.* 1612:1–40.

8. Stopar, D., R. B. Spruijt, C. J. Wolfs, and M. A. Hemminga. 2003. Protein-lipid interactions of bacteriophage M13 major coat protein. *Biochim. Biophys. Acta.* 1611:5–15.

9. Stopar, D., R. B. Spruijt, and M. A. Hemminga. 2006. Anchoring mechanisms of membrane-associated M13 major coat protein. *Chem. Phys. Lipids.* 141:83–93.

10. Fernandes, F., L. M. Loura, M. Prieto, R. Koehorst, R. B. Spruijt, et al. 2003. Dependence of M13 major coat protein oligomerization and lateral segregation on bilayer composition. *Biophys. J.* 85:2430–2441.

11. Marsh, D. 2008. Protein modulation of lipids, and vice-versa, in membranes. *Biochim. Biophys. Acta.* 1778:1545–1575.

12. Morein, S., A. -S. Andersson, L. Rilfors, and G. Lindblom. 1996. Wild-type *Escherichia coli* cells regulate the membrane lipid composition in a "window" between gel and non-lamellar structures. *J. Biol. Chem.* 271:6801–6809.

13. Dong, H., S. E. Paramonov, L. Aulisa, E. L. Bakota, and J. D. Hartgerink. 2007. Self-assembly of multidomain peptides: balancing molecular frustration controls conformation and nanostructure. *J. Am. Chem. Soc.* 129:12468–12472.

14. Meijer, A. B., R. B. Spruijt, C. J. A. M. Wolfs, and M. A. Hemminga. 2001. Membrane-anchoring interactions of M13 major coat protein. *Biochemistry.* 40:8815–8820.

15. Spruijt, R. B., A. B. Meijer, C. J. A. M. Wolfs, and M. A. Hemminga. 2000. Localization and rearrangement modulation of the N-terminal arm of the membrane-bound major coat protein of bacteriophage M13. *Biochim. Biophys. Acta.* 1509:311–323.

16. Spruijt, R. B., C. J. A. M. Wolfs, and M. A. Hemminga. 1989. Aggregation-related conformational change of membrane-associated coat protein of bacteriophage M13. *Biochemistry.* 28:9158–9165.

17. Spruijt, R. B., C. J. M. Wolfs, and M. A. Hemminga. 2004. Membrane assembly of M13 major coat protein: evidence for a structural adaptation in the hinge region and a tilted transmembrane domain. *Biochemistry.* 43:13972–13980.

18. Ahyayauch, H., B. Larijani, A. Alonso, and F. M. Goñi. 2006. Detergent solubilization of phosphatidylcholine bilayers in the fluid state: influence of the acyl chain structure. *Biochim. Biophys. Acta.* 1758:190–196.

19. Koynova, R., and M. Caffrey. 1998. Phases and phase transitions of the phosphatidylcholines. *Biochim. Biophys. Acta.* 1376:91–145.

20. Stopar, D., J. Štrancar, R. B. Spruijt, and M. A. Hemminga. 2005. Exploring the local conformational space of a membrane protein by site-directed spin labeling. *J. Chem. Inf. Model.* 45:1621–1627.

21. Stopar, D., R. B. Spruijt, C. J. A. M. Wolfs, and M. A. Hemminga. 1996. Local dynamics of the M13 major coat protein in different membrane-mimicking systems. *Biochemistry.* 35:15467–15473.

22. Stopar, D., R. B. Spruijt, C. J. A. M. Wolfs, and M. A. Hemminga. 1997. In situ aggregational state of M13 bacteriophage major coat protein in sodium cholate and lipid bilayers. *Biochemistry.* 36:12268–12275.

23. Stopar, D., R. B. Spruijt, C. J. A. M. Wolfs, and M. A. Hemminga. 1998. Mimicking initial interactions of bacteriophage M13 coat protein

disassembly in model membrane systems. *Biochemistry.* 37:10181–10187.

24. Stopar, D., R. B. Spruijt, C. J. A. M. Wolfs, and M. A. Hemminga. 2002. Structural characterization of bacteriophage M13 solubilization by amphiphiles. *Biochim. Biophys. Acta.* 1594:54–63.

25. Wolkers, W. F., R. B. Spruijt, A. Kaan, R. N. H. Konings, and M. A. Hemminga. 1997. Conventional and saturation-transfer ESR of spin-labeled mutant bacteriophage M13 coat protein in phospholipid bilayers. *Biochim. Biophys. Acta.* 1327:5–16.

26. Stopar, D., J. Štrancar, R. B. Spruijt, and M. A. Hemminga. 2006. Motional restrictions of membrane proteins: a site-directed spin labeling study. *Biophys. J.* 91:3341–3348.

27. Koehorst, R. B. M., R. B. Spruijt, F. J. Vergeldt, and M. A. Hemminga. 2004. Lipid bilayer topology of the transmembrane α-helix of M13 major coat protein and bilayer polarity profile by site-directed fluorescence spectroscopy. *Biophys. J.* 87:1445–1455.

28. Vos, W. L., R. B. M. Koehorst, R. B. Spruijt, and M. A. Hemminga. 2005. Membrane-bound conformation of M13 major coat protein: a structure validation through FRET-derived constraints. *J. Biol. Chem.* 280:38522–38527.

29. Vos, W. L., M. Schor, P. V. Nazarov, R. B. M. Koehorst, R. B. Spruijt, et al. 2007. Structure of membrane-embedded M13 major coat protein is insensitive to hydrophobic stress. *Biophys. J.* 93:3541–3547.

30. Veatch, S. L., and S. L. Keller. 2005. Seeing spots: complex phase behavior in simple membranes. *Biochim. Biophys. Acta.* 1746:172–185.

31. Sankaram, M. B., D. Marsh, and T. E. Thompson. 1992. Determination of fluid and gel domain sizes in two-component, two-phase lipid bila-

yers. An electron spin resonance spin label study. *Biophys. J.* 63:340–349.

32. Chandrashekar, I. R., and S. M. Cowsik. 2003. Three-dimensional structure of the mammalian tachykinin peptide neurokinin A bound to lipid micelles. *Biophys. J.* 85:4002–4011.

33. Holte, L. L., S. A. Peter, T. M. Sinnwell, and K. Gawrisch. 1995. ^{2}H nuclear magnetic resonance order parameter profiles suggest a change of molecular shape for phosphatidylcholines containing a polyunsaturated acyl chain. *Biophys. J.* 68:2396–2403.

34. Petrache, H. I., S. W. Dodd, and M. F. Brown. 2000. Area per lipid and acyl length distributions in fluid phosphatidylcholines determined by ^{2}H NMR spectroscopy. *Biophys. J.* 79:3172–3192.

35. Fernandes, F., L. M. S. Loura, R. B. M. Koehorst, R. B. Spruijt, M. A. Hemminga, et al. 2004. Quantification of protein-lipid selectivity using FRET. Application to the M13 major coat protein. *Biophys. J.* 87:344–352.

36. Wickner, W. 1976. Asymmetric orientation of phage M13 coat protein in *Escherichia coli* cytoplasmic membranes and in synthetic lipid vesicles. *Proc. Natl. Acad. Sci. USA.* 73:1159–1163.

37. Shogomori, H., A. T. Hammond, A. G. Ostermeyer-Fay, D. J. Barr, G. W. Feigenson, et al. 2005. Palmitoylation and intracellular domain interactions both contribute to raft targeting of linker for activation of T cells. *J. Biol. Chem.* 280:18931–18942.

38. Brown, D. A. 2006. Lipid rafts, detergent-resistant membranes, and raft targeting signals. *Physiology (Bethesda).* 21:430–439.

39. Strandberg, E., and J. A. Killian. 2003. Snorkeling of lysine side chains in transmembrane helices: how easy can it get? FEBS Lett. 544:69–73.